JAAS

ROYAL SOCIETY OF CHEMISTRY

PAPER

View Article Online
View Journal

Cite this: DOI: 10.1039/d0ja00393j

Gated and non-gated silver detection using microwave-assisted laser induced breakdown spectroscopy

M. A. Wakil and Zeyad T. Alwahabi *

The detection of silver using microwave-assisted laser induced breakdown spectroscopy (MW-LIBS) is demonstrated in solid and liquid samples at a 338.28 nm emission line. For solid sample analysis, the limit of detection (LoD) with a gated detector has been compared with that of a portable spectrometer with a non-gated detector. The LoD achieved by the gated and non-gated detectors are 4.5 ± 1.0 ppm and 7 ± 2.3 ppm, respectively. For aqueous silver, the LoD was found to be 385 ± 51 ppb. The LoD of MW-LIBS is more effective in liquid sample analysis than in solid sample analysis for atomic detection. The accuracy of the established calibration curve, based on the gated detector, has been verified to be ~84%. For MW-LIBS, it was observed that relatively low laser energy is sufficient to develop a calibration curve and achieve an outstanding LoD.

Received 4th September 2020
Accepted 9th November 2020

DOI: 10.1039/d0ja00393j

rsc.li/jaas

1. Introduction

The precise, accurate and fast detection of precious metals is becoming an important aspect of the mining industry, in terms of exploration, development and production. Silver is one of the world's most precious metals of the platinum family with is used in a wide variety of applications such as antimicrobials, disinfectants, biosensor materials, composite fibres, cryogenic superconducting materials, cosmetic products, electrical components, food packaging, functionalized plastics, wound dressings, photographic materials and processing, electroless plating, coating, brazing and soldering uses, *etc.*[1–6] Due to its intensive usage, it is suggested that silver likely ends up in the environment through landfill, wastewater, soil surface, and contamination of surface water by natural leaching caused by bedrock and mining activities. Silver may exist in different oxidation states such as Ag^0, Ag^{1+}, Ag^{2+} and Ag^{3+}.[7] Only a few silver compounds are deemed toxic, for example the silver thiosulfate complex (least toxic) and silver nitrate (most toxic).[8] However, the wastage of silver, given its economic value, requires fast effective detection for proper quantification.

Several analytical techniques involving digestion methods for quantification of precious metals are reported in the literature. They include, for instance, fire assay, wet acid treatment, direct chlorination, alkaline oxidation fusion, *etc.*[9] Maria Balcerzak[9] reviewed all the digestion methods including the advantages and hindrances of these methods. However, only a few detection techniques for silver are reported in the literature such as silver-specific DNA[10] and visual detection based on gold nanoparticles (AuNPs)[11] for silver ions. These techniques are limited to liquid samples and require a long detection time. The laser induced breakdown spectroscopy (LIBS) technique is a promising fast detection technique that may satisfy the requirements of the mining industry due to its substantial unique characteristics such as *in situ*, online and multi-element analysis with minimal or no sample preparation.[12]

However, using LIBS, Daniel *et al.* detected silver in ore samples[13] and reported a limit of detection (LoD) of 1 ppm. R. W. Septianti *et al.*[14] checked the authenticity of silver jewellery and reported a LoD of 2.74%. I. Rehan *et al.*[15] used monosodium glutamate and reported a detection limit of 0.57 ppm. However, there is a limitation to the LIBS technique in that it cannot estimate the extent of metals with complex structures and elements with a high content (due to matrix and self-absorption effects).[16] Poor repeatability is also a significant limitation of LIBS.[16] Another important limitation of LIBS observed by this present study's authors is the need to apply significantly high laser energy for proper signal analysis. For example, Daniel Diaz *et al.* applied 100–180 mJ laser energy in their experiment,[13] and I. Rehan and his group applied about 60 mJ for silver detection in their analysis.[15] The application of high laser energy makes the system more destructive when it is implemented outside the laboratory environment.

The microwave-assisted LIBS technique (MW-LIBS) is a promising technique in that it enables the system to be less destructive because it employs significantly less laser energy. It is reported that the MW-LIBS system is more advantageous than LIBS because of certain benefits, for instance a long plasma lifetime, larger volume, strong emission intensity, better stability and ability to reduce self-absorption.[17,18] For example,

School of Chemical Engineering and Advanced Materials, The University of Adelaide, SA 5005, Australia. E-mail: zeyad.alwahabi@adelaide.edu.au

Viljanen *et al.* observed an approximate 93-fold higher LoD with MW-LIBS compared to LIBS for copper[19] at 2.5 mJ laser energy. Chen *et al.*[20] reported a 3.38 μg g^{-1} limit of copper detection, using Near Field Applicator (NFA) microwave devices. Wall *et al.* reported an 11.5-fold enhanced LoD for indium at a laser pulse fluence of 85.2 J cm^{-2}.[21] Al Shuaili *et al.*[22] established an 8-fold improved LoD with MW-LIBS for palladium at 650 J cm^{-2}. Similarly, Khumaeni *et al.*[23] reported about a 32-fold enhancement for gadolinium (Gd) at 5 mJ laser energy.

This work focusses on the evaluation of MW-LIBS for silver detection in a laboratory under ambient conditions in solid and liquid phases. The study will be carried out with two spectrometers, namely a spectrometer with an ICCD camera and a portable small spectrometer without an ICCD at low laser energy. The focus is comparing the detection limit using both the spectrometers with MW-LIBS in order to make the system compatible with practical conditions outside the laboratory. The experiment includes microwave dependence on the signal-to-noise ratio (SNR), plasma temperature and electron density measurement and quantitative detection of silver. The calibration curve and the LoD was obtained using standard ore samples with different contents of silver.

2. Methodology

2.1 MW-LIBS experimental setup

A schematic diagram of the MW-LIBS experimental setup is presented in Fig. 1(a) and (b) for solid and liquid detection, respectively. A Q-switch second order harmonic Nd:YAG laser with a wavelength of 532 nm was utilized as a light source. The pulse width was ~6 ns with a repetition of 10 Hz. A combined half-wave plate (HWP) and Glan-laser polarizer (P) were used for

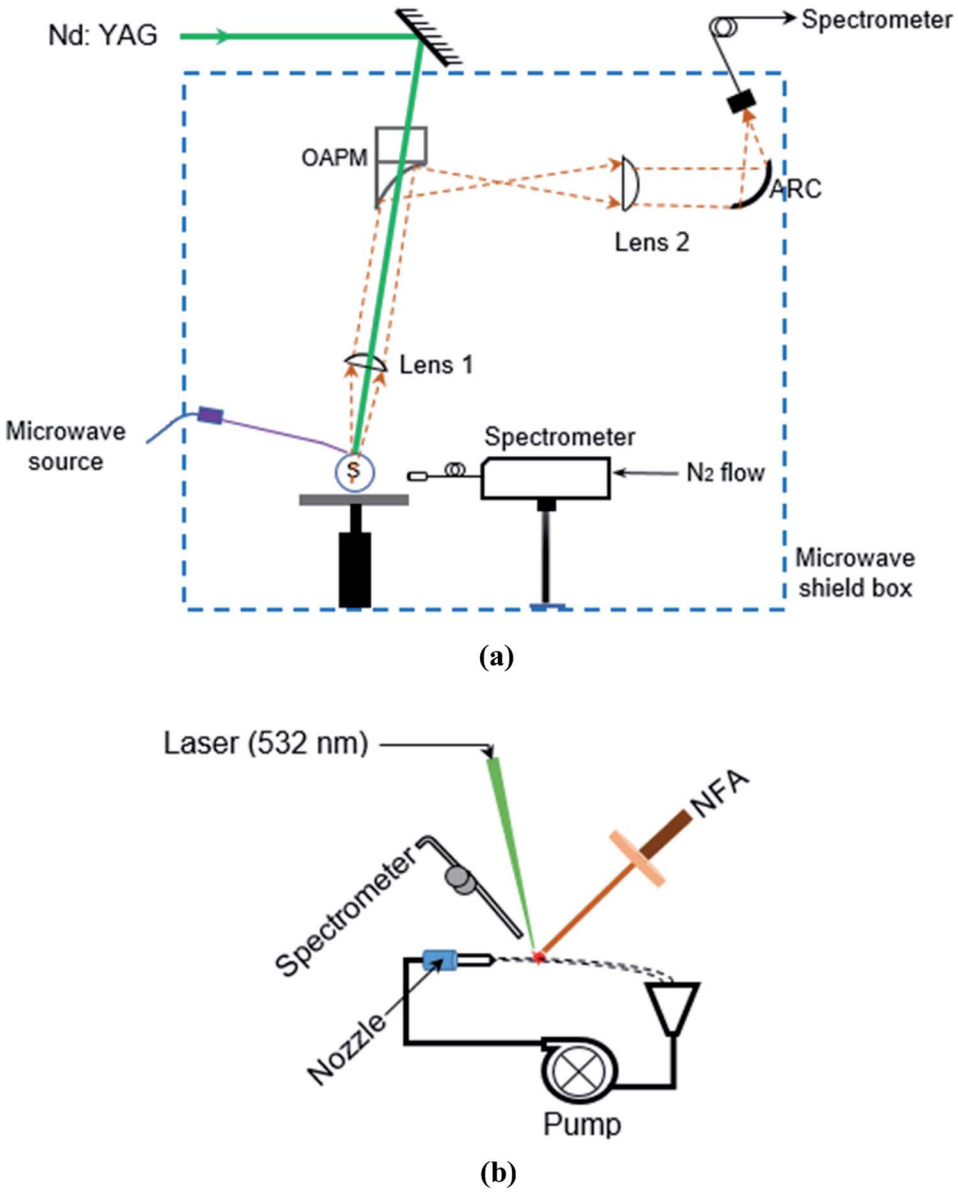

Fig. 1 (a) Schematic diagram of the experiment for solid silver. (b) Schematic diagram of the experiment for liquid silver.

controlling the ablation pulse energy. The laser energy was measured with a Pyroelectric sensor (ES 220C). The laser beam was allowed to pass along the sample surface by a dichroic mirror (DM) with a high reflectivity in the spectral range of 500–550 nm. Then the beam was focussed on the sample surface using a fused silica lens (with $f = 100$ mm). The propagation of the laser beam was at a 15° angle to the vertical surface and the spot size was estimated to be 7.32 μm. In this experiment, 2 mJ laser energy was considered, while 1–3 mJ laser energy was used for the smallest amount of laser energy in our experiment. To achieve ablation from the fresh sample surface for each shot, the sample was placed on a rotating disk at an angular velocity of 7 revolutions per minute. A second continuous-wave (CW)[24] laser armed with a camera served to monitor the uniform height between the sample and laser beam with a camera connected to a display unit.

For liquid samples, a steady liquid circulation system was used. To achieve this, a peristaltic pump (Ismatec, MW-MSC 1), a 25 ml syringe as a sample reservoir, a circular nozzle with a 0.8 mm diameter and a collection funnel were connected to rubber-plastic tubing (Masterflex 6485-16). This process created a liquid circulation system as shown in Fig. 1(b). At 360 rpm of pump operation, ~50 ml solution from liquid samples was periodically added to the syringe in order to avoid any bubble in the liquid circulation system. The operating flow rate was chosen to create a stable horizontal liquid jet (70 ml min^{-1}). The laser incident was at an angle of 15° to the vertical surface. It is worth noting that distilled water was used to wash out the Ag sample in the flow to avoid contamination after each analysis.

A water-cooled 3000-Watt Sairem microwave system was utilized with a frequency of 2.45 GHz (GMP30KIP56T400F-ST3IR). The microwave was directed *via* a WR340 waveguide to a 3-stub impedance tuner (AI3SMWR340D24X25MRR2PE) and then to a waveguide-to-coaxial adaptor (WR340RN) through a quartz window. The waveguide-to-coaxial adaptor was connected to an NFA device by a 1 m flexible coaxial cable (50 Ω NN cable) with 0.14 dB@2.45 GHz. The design details of the NFA have been reported by Chen *et al.*[20] To avoid possible silver contamination from the coating of the NFA core wire, a pure platinum wire (99.9%) was soldered to the end of the NFA. The tip of the NFA was positioned approximately 1 mm and 0.5 mm vertically above the sample surface and horizontally away from the ablation spot, respectively. The microwave pulse duration and microwave power were controlled with an analogue signal from an Aim-TTi type pulse generator. For the solid matrix and for the liquid matrix, 450 W and 1200 W microwave power was used respectively at pulse duration of 1.5 ms.

To analyse the plasma emission resulting from ablation, two spectrometers were employed, namely the gated (a spectrometer with an ICCD) and non-gated (a spectrometer without an ICCD) types.

For the gated detection, the plasma emission was collected directly through a perforated parabolic mirror (FL = 152 mm) and then focussed by a plano-convex lens (FL = 100 nm), onto the sample by a plano-convex UV fused silica lens with a focal length of 100 mm and a diameter of 50.8 mm. The emission was collimated by a plano-convex lens (FL = 100 nm) and then focused by an off-axis parabolic mirror (OAPM). A second lens (FL = 20 mm) coupled the emission onto an Achromatic Reflective Coupler (ARC), which is connected to a 7-fibre bundle (Thorlabs, BFL200HS02). The fibre bundle was a round-to-linear bundle, 7× Ø 200 μm core. The spectrometer (Andor Shamrock 500i) with a grating of 2400 lines per mm has a spectral resolving power of 10 000, *i.e.*, the spectral resolution is 0.031 nm in the 320–332 nm spectral range. An intensified CCD camera (Andor, iStar) recorded the spectral signal, which was then synchronized with the laser and the microwave generator with an external signal delay box (Princeton Technology Corporation). In this study, the microwave pulse duration was kept constant at 1.5 ms.

Referring to non-gated spectrometry, the plasma emission was collected by a 600 μm, 0.25 m long, solarisation-resistant fibre. The fibre, placed 20 mm away from the plasma, was connected to a Mayo2000-Pro (Ocean Optics) equipped with a 25 μm entrance slit and nitrogen gas purge port. The spectrometer had a vacuum deep UV mirror and a UV holographic grating with a groove density of 1200. Spectra were recorded by a windowless and back-illuminated uncooled detector (Hamamatsu S10420). The detector contains 2048 × 64 active pixels and has a quantum efficiency of 60% at 250 nm. This configuration has improved the light collection efficiency and signal-to-noise ratio significantly. The integration time was fixed at 8 ms for this spectrometer with wavelengths ranging from 179 nm to 400 nm.

Table 1 Silver concentration in this study

Element	Concentration (ppm), solid	Standard deviation (σ)	Concentration (ppm), liquid
Silver (Ag)	58	5	10
	209	59	20
	416	16	50
	493	49	70
	527	29	100
	1373	84	150
	—	—	200
	—	—	500

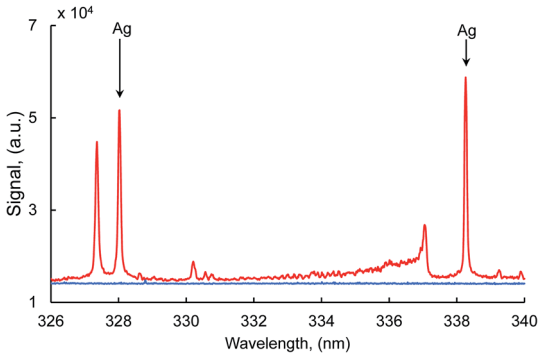

Fig. 2 Typical MW-LIBS silver signal from the certified ore sample at 2 mJ laser energy, 450 W microwave power, 1 ns gate-delay, 1000 us gate-width with an average of 30 shots, LIBS (blue), and MW-LIBS (red).

2.2 Samples

The study was carried out with solid ore samples and a high purity standard of 1% liquid silver for calculating the silver detection limit. Certified reference materials from GEOSTATS Mining Industry Consultants Reference Material Manufacture and Sales were purchased, namely, GBC915-3, GBC616-2, GLC915-1, GBC916-3, GLC316-2, and GLC615-6. These samples contained silver of different certified concentrations (58 ± 5 ppm–1373 ± 84 ppm). All the samples were made by mixing the supplied samples with distilled water and organic binder. All the samples were prepared as disks (20.45 ± 0.1 mm dia. and 1.8 ± 0.02 mm thick) by simple green compacting using an aluminium holder that were best suited for the rotating disk. The liquid silver of 1% was purchased from Choice Analytical for analysis purposes. The liquid samples of different concentrations (10 ppm–500 ppm) were prepared by diluting the pure sample with distilled water. Silver concentrations used in solid and liquid detection have been shown in Table 1.

3. Results and discussion

3.1 Spectral information

Typical silver atomic lines recorded using MW-LIBS are presented in Fig. 2. Silver (AgI) has two strong transition lines at 328.06 nm and 338.28 nm with the same transition $5P\ ^2P^0 \rightarrow 5S$

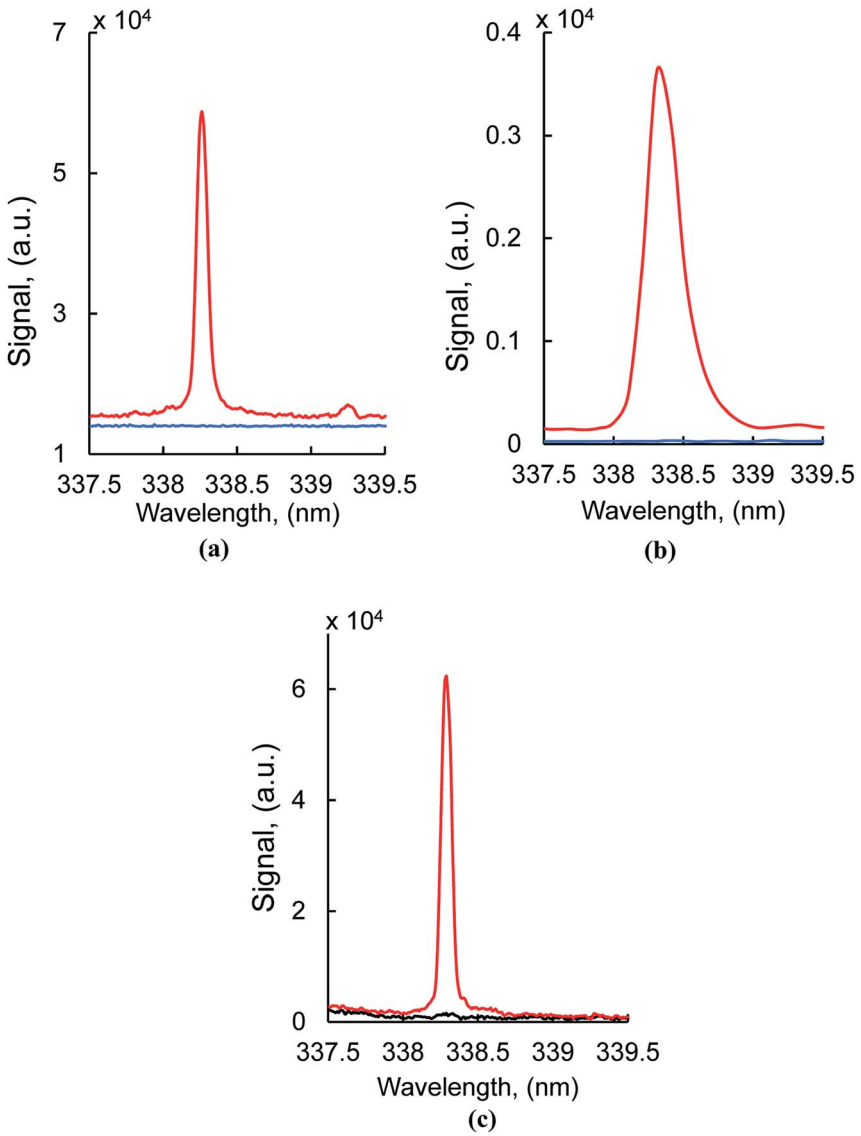

Fig. 3 (a) Signal from 1373 ppm Ag containing samples at 2 mJ laser energy, 450 W microwave power, recorded with a gated detector of 1 ns gate-delay, 1000 μs gate-width with an average of 30 shots, LIBS (blue), and MW-LIBS (red). (b) Signal from 1373 ppm Ag containing samples at 2 mJ laser energy, 450 W microwave power and 8 ms integration time recorded with a non-gated detector with integration time with an average of 30 shots, LIBS (blue), and MW-LIBS (red). (c) Typical MW-LIBS signal of the 500 ppm Ag containing liquid sample at 10 mJ laser energy, 1200 W microwave power, recorded with a gated detector at 2 μs gate-delay, 500 μs gate-width with an average of 100 shots, distilled water (black), and 500 ppm [Ag] (red).

^{2}S, which is between 0.0 cm^{-1} to 30472.66 cm^{-1} and 0.00 cm^{-1} to 29552.05 cm^{-1}. Copper has a very strong line at 327.4 nm which is closer to 328.0 nm (AgI) as shown in Fig. 2. For that reason, the line at 328.06 nm was not considered for this study. The experimental analysis was continued for both LIBS and MW-LIBS with two different spectrometers (variable configurations) but at relatively low laser energy (2 mJ), LIBS did not give any visible spectra for Ag at 338.28 nm as shown in Fig. 3(a) and (b). It is seen from Fig. 3 that the signal with the portable non-gated spectrometer is smaller (Fig. 3(b)) than when employing the gated spectrometer (Fig. 3(a)). This may be due to the gated spectrometer's detector gain. The aim of this study was to determine the spectra at very low laser energy. At 2 mJ, MW-LIBS shows sufficient signal strength for calculating the limit of detection (LoD). Fig. 3(c) shows the silver spectra in the liquid phase. To check the contamination of silver from distilled water, the experiment was conducted for distilled water utilizing the same operating conditions that are illustrated in Fig. 3(c) (black). It was observed that no contamination of silver from distilled water occurred. The experiment for liquid silver was conducted at 10 mJ laser energy, which was higher than the laser energy in the solid phase because of inconsistent laser plasma below 10 mJ in liquid samples. Fig. 4(a) and (b) show the sample emission spectra of AgI at 338.28 nm for different concentrations of Ag with MW-LIBS in solid and liquid silver containing samples, respectively.

3.2 Signal to noise ratio measurement

To justify the operating conditions used for calculating the limit of detection, the dependence of microwave power on laser energy was investigated for an optimized signal-to-noise ratio (SNR). Fig. 5(a) and (b) present the silver SNR with solid and liquid samples, respectively. It is seen from Fig. 5 that, at very low laser energy, there is a sufficient SNR with MW-LIBS, where there is no signal with LIBS only both in the solid (1–3 mJ) and liquid (5–10 mJ), respectively. This is due to the signal microwave system's enhancing ability. The external energy supplied, using the microwave radiation, will sustain free electrons present within the laser induced plasma. These reenergized free electrons act as an excitation source, *via* collisional processes, leading to an extended life, which in turn finally results in signal enhancement.[21,25] Fig. 5(a) shows that the increase in the SNR with increasing MW power in solid samples differs slightly from the liquid samples. For the solid sample, the SNR increases until 600 W is reached and beyond this figure there is no significant impact of microwave power on the SNR. The same result was documented in our paper on chlorine[26] and an unpublished report on sulphur. On the other hand, microwave power wields a significant impact on the SNR in the case of liquid samples as shown in Fig. 5(b). There is always an increasing order of the SNR when the microwave power also increases. A microwave power below 600 W has not been considered in this study due to the instability of the microwave plasma. The other reason for the weaker plasma from LIBS is explained by the reflective nature of the thin water jet, which requires more microwave power for proper coupling with the LIBS plasma. The results published by Matthew Wall *et al.*[21] support our experimental outcomes. A laser energy below 5 mJ is not suitable for plasma formation in a liquid jet.

3.3 Plasma temperature and electron density measurement

To study the MW-LIBS plasma, detailed information about plasma parameters is required. Considering the local thermodynamic equilibrium (LTE), the plasma temperature was measured using Boltzmann plots.[27] Plasma temperature in the solid matrix has been measured in our accepted article.[28] To measure the plasma temperature for the liquid matrix four strong lines of CaI were used. The spectral information

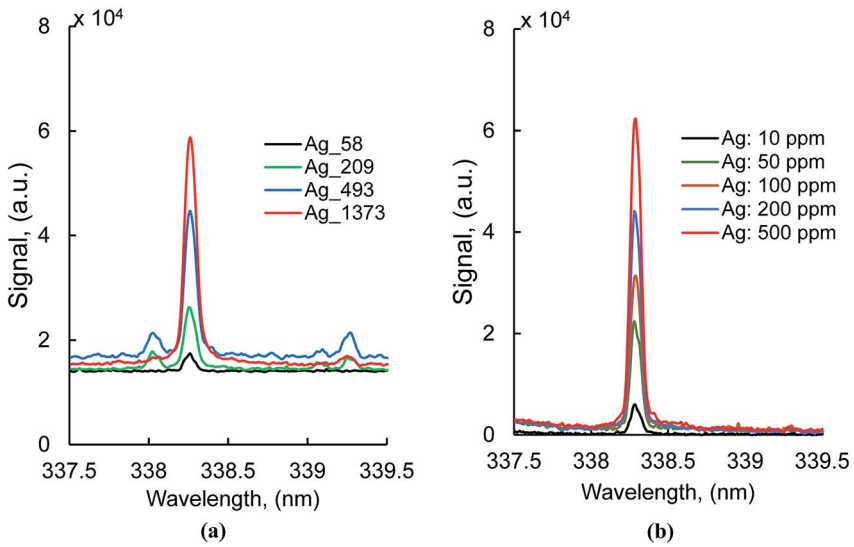

Fig. 4 (a) Typical spectra of the MW-LIBS signal of different silver concentrations from certified ore samples at 2 mJ, 450 W, 1 ns gate-delay and 1 ms gate-width. (b) Typical spectra of the MW-LIBS signal of different concentrations with liquid samples at 10 mJ, 1200 W, 2 μs gate-delay and 500 μs gate-width.

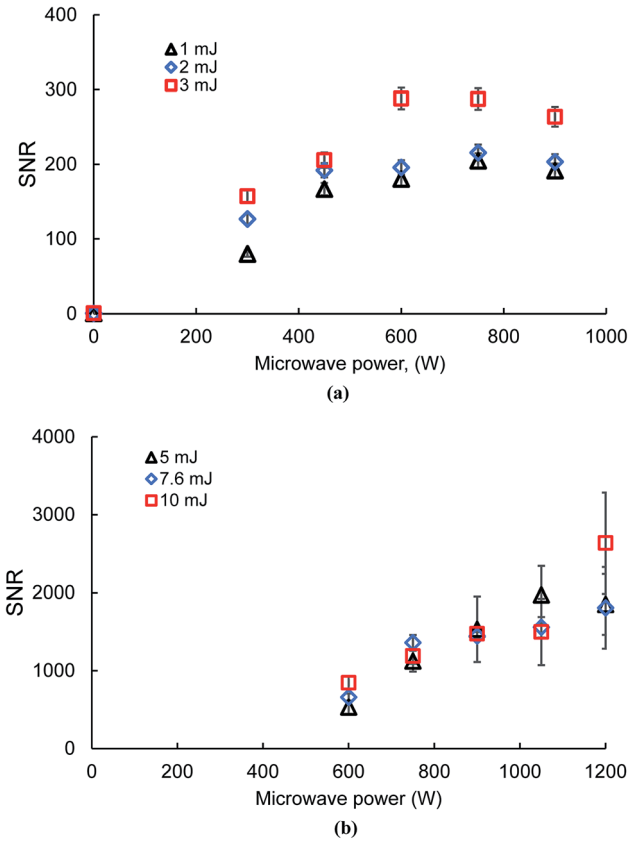

Fig. 5 (a) Signal to noise ratio (SNR) for the solid sample with 1373 ppm [Ag] at 150 μs gate-delay, 500 μs gate-width and 30 shots. (b) Signal to noise ratio (SNR) for the liquid sample with 1000 ppm [Ag] at 1 ns gate-delay, 1000 μs gate-width and 50 shots.

from NIST for plasma temperature measurement is given in Table 2. The Boltzmann plots using CaI lines are shown in Fig. 6. The plasma temperature calculated for the liquid matrix using MW-LIBS was 4122 ± 192 K at 10 mJ and 1200 W. This analysis employed a minimum laser energy and microwave power for silver detection. For the solid sample, 2 mJ laser energy with 450 W microwave power gave a sufficient SNR for developing the calibration curve but for the liquid, and we employed 10 mJ laser energy with 1200 W microwave power. The reason for using relatively high laser energy and high microwave power is to ensure a consistent MW-LIBS plasma.

The recommended spectral line for electron density calculation is a well-isolated spectral line of hydrogen at 656.279 nm.

Table 2 Spectroscopic data of calcium (CaI)[29]

Wavelength (nm)	A_{ki} (s^{-1})	E_k (eV)	g
364.44	3.55×10^7	5.3	7
422.67	2.18×10^8	2.93	3
430.25	1.36×10^8	4.779	5
445.48	4.70×10^7	4.681	7

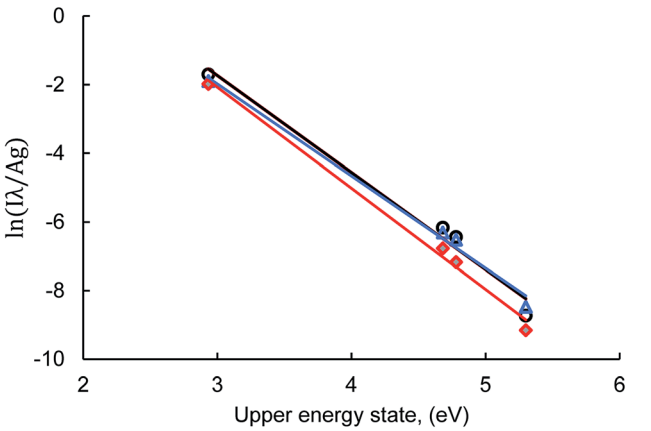

Fig. 6 Boltzmann plot made from CaI lines at 10 mJ laser energy, 1200 W microwave power, 2 μs gate-delay, and 500 μs gate-width.

The plasma electron density in the liquid can be calculated using the relationship of full-width-half-maximum (FWHM) and electron density as expressed by Ashkenazy *et al.*[30] as

$$N_e(H_\alpha) = 8.02 \times 10^{12} \times (\mathrm{FWHM}/\alpha_{1/2})^{3/2}\ \mathrm{cm}^{-3} \quad (1)$$

However, the half width of the reduced stark profile ($\alpha_{1/2}$) is temperature sensitive and all the $\alpha_{1/2}$ values reported in the literature were above 10 000 K,[31] The Ca 422.59 nm line has been used to evaluate the electron density. In this case, the plasma electron density was calculated using the relationship of full-width-half-maximum (FWHM) and electron density as expressed by Harilal *et al.*[32] A well-isolated CaI line at 422.6 nm has been chosen because this line exhibits quadratic stark broadening. The stark width broadening parameter for CaI at 422.6 nm was considered as 1.12×10^{-6} Å.[33] The full-width at half-maximum (FWHM) was measured using the stark broadened calcium line as depicted in Fig. 7. The FWHM was corrected by subtracting the instrumental broadening. The instrumental broadening was measured to be 0.0321 by recoding the Hg line at 253.6 nm. The electron density measured for the liquid plasma was 3.874×10^{16} cm^{-3} at a laser energy and microwave power of 10 mJ and 1200 W, respectively. To understand if the plasma is at local thermodynamically equilibrium (LTE), the McWhirter criterion was calculated using eqn (2).[34] For the liquid plasma the lower limit of electron density was 1.51×10^{16} cm^{-3} considering $\Delta E = 5.3$ eV and $T = 4122$ K. These values are much lower than the electron densities calculated for the solid and liquid samples, which substantiates the LTE conditions:

$$N_e \geq 1.6 \times 10^{12} \Delta E^3 T_e^{1/2} \quad (2)$$

3.4 Quantitative detection of silver

Calibration curves were generated using the MW-LIBS signal for both solid and liquid matrices. Calibration curves were developed using the strong silver line at 338.28 nm. For calculating

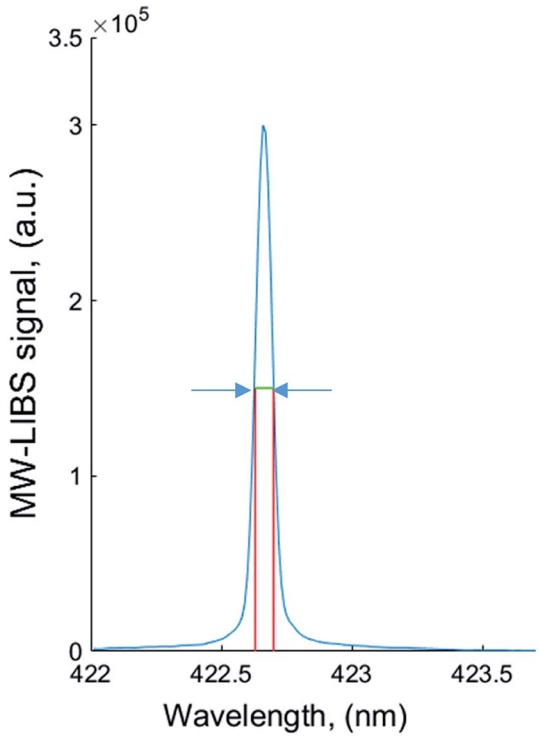

Fig. 7 Typical example of full width at half-maximum of CaI at 422.6 nm in the liquid sample at 10 mJ laser energy and 1200 W microwave power.

the LoD in solid and liquid phases, the experimental conditions were different.

3.4.1 LoD of silver in the solid phase. For the certified ore sample, the experimental conditions were 2 mJ laser energy, 450 W microwave power, 1 ns gate-delay, and 1 ms gate-width with an accumulation of 30 shots. Fig. 8(a) shows the calibration curve for solid silver with a gated spectrometer. The LoD was calculated using the 3-sigma method[35,36] and found to be 4.5 ± 1.0 ppm LoD. The same experiment was done with a non-gated portable spectrometer as shown in Fig. 8(b), and here the LoD was 7 ± 2.3 ppm. It was evident that a portable spectrometer can detect silver with MW-LIBS, which helps to make the experimental system portable for outside uses. The LoD was calculated for liquid silver samples by developing the calibration curve.

3.4.2 LoD of silver in the liquid phase. Fig. 8(c) shows the calibration curve for liquid silver at 10 mJ laser energy and 1200 W microwave power. What emerged was an improved LoD of silver in the liquid matrix that was better than that in the solid matrix. The relatively lower noise in the liquid phase with MW-LIBS is the main reason for the improved LoD. The LoD found in liquid samples was 385 ± 51 ppb.

However, studies[13–15] have been undertaken for the detection of silver as discussed in the Introduction section. To the best of our knowledge, the best LoD for silver was reported by Rehan *et al.*[15] using silver containing salt samples. They reported the LoD as 0.57 ppm which is lower than our present study of 4.5 ppm, but they employed high laser energy (60 mJ), while our

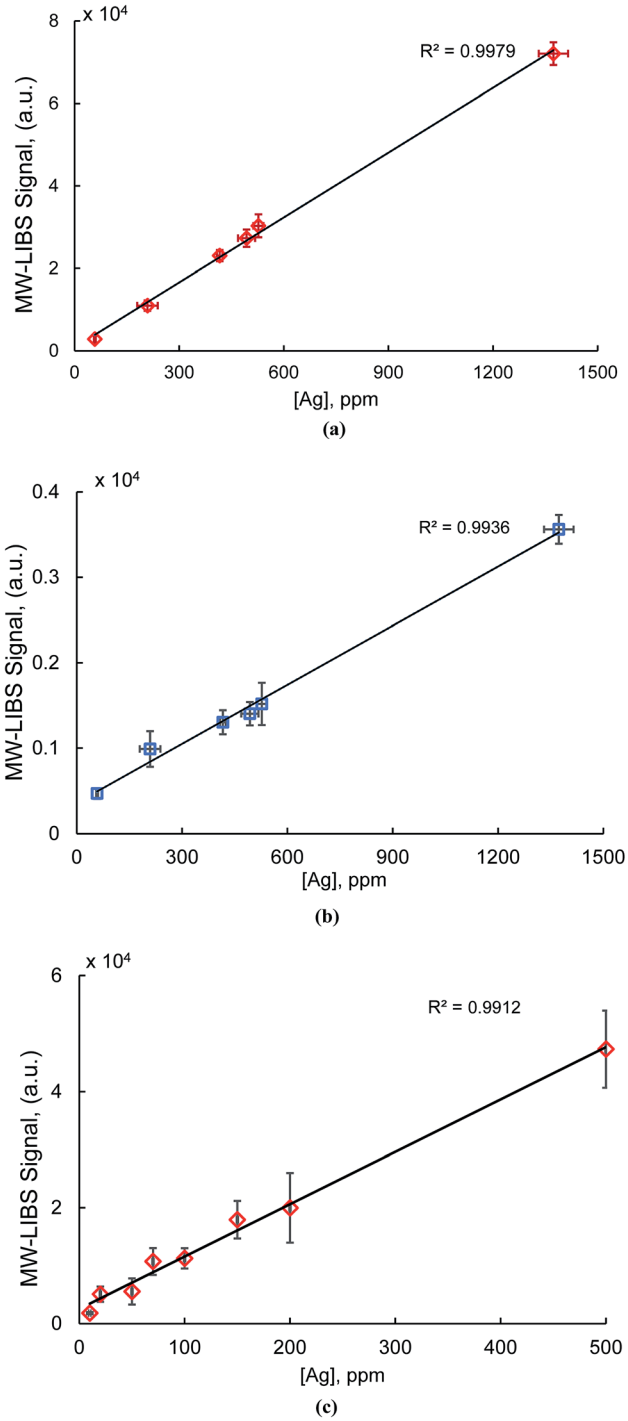

Fig. 8 (a) Calibration curve of silver in the solid matrix obtained with MW-LIBS at 2 mJ laser energy, 450 W microwave power, 1 ns gate-delay, and 1 ms gate-width with an accumulation of 30 single shots. (b) Calibration curve of silver in the solid matrix obtained with MW-LIBS at 2 mJ laser energy, 450 W microwave power, 2.5 ms microwave pulse duration and 8 ms integration time with an accumulation of 30 single shots. (c) Calibration curve of silver in the aqua phase obtained with MW-LIBS at 10 mJ laser energy, 1200 W microwave power, 2 μs gate-delay, and 500 μs gate-width with an accumulation of 50 single shots.

experiment was conducted with only 2 mJ laser energy. To the best of our knowledge, our study is the first to report silver detection in liquid samples with MW-LIBS. Paing *et al.* reported

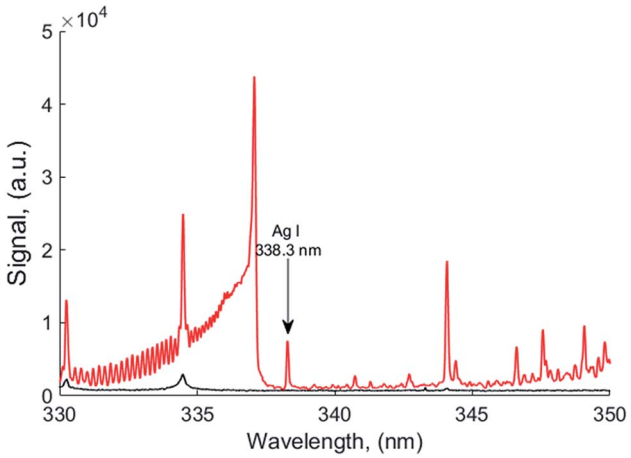

Fig. 9 MW-LIBS (red) and LIBS (black) signals of the real life ORE sample OREAS 351 with an accumulation of 100 single shots.

3.1 ppm silver detection in a liquid *via* the liquid sampling-atmospheric glow discharge optical emission spectroscopy (LS-APGD-OES) method.[37]

3.4.3 Demonstration of calibration curves. Although the calibration curve was generated for solid silver detection using ore samples supplied by GEOSTATS Mining Industry Consultants Reference materials, it has been verified with another set of ore samples using a gated spectrometer. The sample was supplied by OREAS as a certified reference material named OREAS 351. Fig. 9 shows clearly the MW-LIBS silver signal of the OREAS 351 sample at 338.3 nm. Using the calibration curve of Fig. 8(a), the concentration has been calculated to be 101 ppm for the OREAS 351 sample. The OREAS Company certified the Ag concentration in the OREAS 351 sample as 120 ppm, based on the 4-Acid digestion method. This shows ~84% accuracy of the established calibration curve.

4. Conclusion

Quantitative silver detection with gated and non-gated spectrometers using the microwave-assisted LIBS technique is reported for the first time. Silver detection has been described here for solid and liquid samples. The limit of detection with a laboratory-scale gated spectrometer was compared to that of a portable non-gated spectrometer. The MW-LIBS technique is more sensitive in the liquid than in the solid for achieving a superior detection limit. The experimental study was carried out at a very low laser energy, the objective being to establish the effectiveness of MW-LIBS when compared to LIBS. It has been shown that MW-LIBS is able to achieve a strong signal with low laser energy, yet LIBS is unable to detect any signal by using silver at 338.28 nm. The limit of detection reported in this study is 4.5 ± 1.0 ppm in the solid and 0.385 ± 0.051 ppm in the liquid. The detection limit of silver is also calculated using a portable spectrometer at 7 ± 2.3 ppm. The calibration curve, based on the gated spectrometer, has been verified using another certified ore sample with ~84% accuracy.

Conflicts of interest

There are no conflicts to declare.

References

1 P. Verma and S. K. Maheshwari, *Int. J. Nano Dimens.*, 2019, **10**, 18–36.
2 T. W. Purcell and J. J. Peters, *Environ. Toxicol. Chem.*, 1998, **17**, 539–546.
3 S. Senapati, PhD thesis, Savitribai Phule Pune University, 2005.
4 T. Klaus-Joerger, R. Joerger, E. Olsson and C.-G. Granqvist, *Trends Biotechnol.*, 2001, **19**, 15–20.
5 J. Fabrega, S. N. Luoma, C. R. Tyler, T. S. Galloway and J. R. Lead, *Environ. Int.*, 2011, **37**, 517–531.
6 C. Zhang, Z. Hu and B. Deng, *Water Res.*, 2016, **88**, 403–427.
7 E. McGillicuddy, I. Murray, S. Kavanagh, L. Morrison, A. Fogarty, M. Cormican, P. Dockery, M. Prendergast, N. Rowan and D. Morris, *Sci. Total Environ.*, 2017, **575**, 231–246.
8 H. T. Ratte, *Environ. Toxicol. Chem.*, 1999, **18**, 89–108.
9 M. Balcerzak, *Sample Digestion Methods for the Determination of Traces of Precious Metals by Spectrometric Techniques*, 2002.
10 K. Jang, J. You, C. Park and S. Na, *New J. Chem.*, 2017, **41**, 1840–1845.
11 B. Liu, H. Tan and Y. Chen, *Microchim. Acta*, 2013, **180**, 331–339.
12 *Laser Induced Breakdown Spectroscopy*, ed. A. Miziolek, V. Palleschi and I. Schechter, Cambridge University Press, Cambridge, 2006, DOI: 10.1017/CBO9780511541261.
13 D. Díaz, D. W. Hahn and A. Molina, *Spectrochim. Acta, Part B*, 2017, **136**, 106–115.
14 R. W. Septianti, W. S. Budi, H. Sugito and A. Khumaeni, in *7th International Seminar on New Paradigm and Innovation on Natural Science and its Application*, ed. B. Warsito, S. P. Putro and A. Khumaeni, Iop Publishing Ltd, Bristol, 2018, vol. 1025.
15 I. Rehan, M. A. Gondal and K. Rehan, *Appl. Opt.*, 2018, **57**, 3191–3197.
16 D. A. Cremers and L. J. Radziemski, in *Laser Induced Breakdown Spectroscopy*, ed. A. W. Miziolek, I. Schechter and V. Palleschi, Cambridge University Press, Cambridge, 2006, pp. 1–39, DOI: 10.1017/CBO9780511541261.002.
17 Y. Ikeda and R. Tsuruoka, *Appl. Opt.*, 2012, **51**, B183–B191.
18 Y. Tang, J. Li, Z. Hao, S. Tang, Z. Zhu, L. Guo, X. Li, X. Zeng, J. Duan and Y. Lu, *Opt. Express*, 2018, **26**, 12121–12130.
19 J. Viljanen, Z. Sun and Z. T. Alwahabi, *Spectrochim. Acta, Part B*, 2016, **118**, 29–36.
20 J. Chen, A. Iqbal, M. Wall, C. Fumeaux and Z. T. Alwahabi, *J. Anal. At. Spectrom.*, 2017, **32**, 1508–1518, DOI: 10.1039/C7JA00046D.
21 M. Wall, Z. W. Sun and Z. T. Alwahabi, *Opt. Express*, 2016, **24**, 1507–1517.
22 A. A. Al Shuaili, A. M. Al Hadhrami, M. A. Wakil and Z. T. Alwahabi, *Spectrochim. Acta, Part B*, 2019, **159**, 105666.

23 A. Khumaeni, T. Motonobu, A. Katsuaki, M. Masabumi and W. Ikuo, *Opt. Express*, 2013, **21**, 29755–29768.
24 M. Bahreini, B. Ashrafkhani and S. H. Tavassoli, *Appl. Phys. B: Lasers Opt.*, 2014, **114**, 439–447.
25 Y. Liu, B. Bousquet, M. Baudelet and M. Richardson, *Spectrochim. Acta, Part B*, 2012, **73**, 89–92.
26 M. A. Wakil and Z. T. Alwahabi, *J. Anal. At. Spectrom.*, 2019, **34**(9), 1892–1899.
27 J. Zalach and S. Franke, *J. Appl. Phys.*, 2013, **113**, 043303.
28 M. A. Wakil and Z. T. Alwahabi, *J. Anal. At. Spectrom.*, 2020, **35**(11), 2620–2626.
29 J. Reader, C. H. Corliss, W. L. Wiese and G. A. Martin, *Wavelengths and Transition Probabilities for Atoms and Atomic Ions : Part I. Wavelengths - Part II. Transition Probabilities*, National Bureau of Standards, NSRDS; NIST researchlibrary; fedlink; americana, 1980.
30 J. Ashkenazy, R. Kipper and M. Caner, *Phys. Rev. A*, 1991, **43**, 5568–5574.
31 P. Kepple and H. R. Griem, *Phys. Rev.*, 1968, **173**, 317–325.
32 S. Harilal, C. Bindhu, R. Issac, V. P. N. Nampoori and C. Vallabhan, *J. Appl. Phys.*, 1997, **82**, 2140–2146.
33 M. S. Dimitrijevic and S. Sahal-Brechot, *Serb. Astron. J.*, 2000, **161**, 39.
34 R. W. P. McWhirter, Plasma Diagnostic Techniques, ed. R. H. Huddlestone and S. L. Leonard, *Library of Congress Catalog Card Number 65-22763*, Academic Press, New York, 1965, p. 201.
35 S. Rosenwasser, G. Asimellis, B. Bromley, R. Hazlett, J. Martin, T. Pearce and A. Zigler, *Spectrochim. Acta, Part B*, 2001, **56**, 707–714.
36 D. W. Hahn and N. Omenetto, *Appl. Spectrosc.*, 2012, **66**, 347–419.
37 H. W. Paing, K. A. Hall and R. K. Marcus, *Spectrochim. Acta, Part B*, 2019, **155**, 99–106.